

Self-consistent description for x-ray, Auger electron, and nuclear excitation by electron transition processes

Yu-kun Ho*

*China Center of Advanced Science and Technology (World Laboratory), P.O. Box 8730, Beijing 100080, China
and Physics Department II, Fudan University, Shanghai 200433, China*

Zhu-shu Yuan, Bao-hui Zhang, and Zheng-ying Pan
Physics Department II, Fudan University, Shanghai 200433, China

(Received 25 January 1993)

The physical processes about x-ray emission, Auger electron emission, and nuclear excitation by electron transition (NEET) induced by deexcitations of the excited atomic states, e.g., the inner shell hole states, are studied self-consistently in the unified nonrelativistic quantum mechanics framework. The emphasis is on exploring the NEET process and its interference with the other two processes. The transition probabilities of these deexcitation channels are given in analytical forms. The numerical calculations for $^{189}_{76}\text{Os}$, $^{197}_{79}\text{Au}$, and $^{237}_{93}\text{Np}$ have been done and compared with the available experimental results.

PACS number(s): 23.20.Js, 23.20.Nx, 32.90.+a

I. INTRODUCTION

A high-energy electron beam, ion beam, or γ -ray may induce ionizations of electrons in inner shells of atoms. These excited atomic states, the inner shell hole states, may decay through three channels: (1) X-ray emission. In this process, an electron in a higher-energy level transits and fills the hole with a photon emission, as illustrated in Fig. 1(a). (2) Auger electron emission. In this process, the electron in high level fills the hole and ionizes another outer shell electron via a virtual photon exchange, as illustrated in Fig. 1(b). (3) NEET (nuclear excitation by electron transition) process [1]. When the required conditions (energies and angular momentums of initial and final states of the electron and nucleus) are satisfied, the electron and nucleus may interact with each other via a virtual photon exchange, and as a result, the electron transits to the hole and the nucleus is excited. Figure 1(c) shows this process.

There are a number of theoretical studies on the NEET process [2-8], which were reviewed by Tkalya in Ref. [6]. Our previous paper [7] investigated the NEET process and presented a formula for calculating its probability. Also, the precise descriptions of the x ray and Auger electron processes are a well-known part of modern atomic physics [9,10]. However, in previous studies the NEET process was studied separately from the others, though the above three processes take place concurrently. Therefore, it is desirable to investigate the three processes based on a unified framework and to explore their in-

terference effects with an emphasis on the NEET process. This is the major objective of the present work. In this study, we use nonrelativistic quantum mechanics and the perturbation method to describe the three processes, x-ray emission, Auger electron emission, and NEET, in the unified theoretical framework as three competing decay channels induced by the deexcitations of excited atomic states. It should be noted that we do not try to calculate the precise probabilities of these processes, but explore the competitive and interference effects of the three decay channels. Also, the NEET studies are still in the early stage of evaluating the order of magnitude. Therefore some approximations, such as the nonrelativistic, point nucleus charge and hydrogenlike atomic wave function approximations, which are obviously too coarse to make any precise calculations for these processes, are adopted in this paper. Sec. II constitutes the unified formalism and derives the formulas for calculating the probabilities of these three processes. Using the formulas, the numerical calculations for $^{189}_{76}\text{Os}$, $^{197}_{79}\text{Au}$, and $^{237}_{93}\text{Np}$ have been done and compared with the available theoretical and experimental results in Sec. III. Section IV is a brief summary.

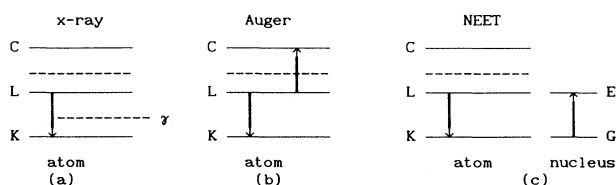


FIG. 1. The deexcitation processes of the atomic hole state. K and L refer to the atomic shell states, and C to the continuum state, while E and G refer to the nuclear excited and ground states, respectively.

*Mailing address: Physics Department II, Fudan University, Shanghai 200433, China.

II. FORMALISM

We use the nonrelativistic quantum perturbation theory to deal with the three processes induced by deexcitation of the atomic hole state. X-ray emission corresponds to the first-order perturbation process, in which the initial state is the atomic hole state and the final state is a hole-filled state plus an emitted real photon. The Auger electron emission and NEET correspond to the second-order perturbation processes, where the final states contain a free Auger electron or an excited nucleus, respectively. There are three intermediate states. (1) Electron 1 is in its final state, and electron 2 and nucleus are in their initial states. This intermediate state links the two-step process. In the first step, electron 1 makes a transition to its final state with a photon emission and in the second step electron 2 or the nucleus absorbs the photon and is excited to its final state. (2) Electron 1 and the nucleus are in their initial states and electron 2 is in its final (excited) state. This links the two-step process, in which the first step electron 2 makes a transition to its final state with a photon and in the second step electron 1 absorbs this photon and makes a transition to its final state. (3) Both electrons 1 and 2 are in their initial states and the nucleus is in its final state. The third intermediate state links the two-step process as follows: In the first step, the nucleus makes a transition to its final state with a photon, and in the second step electron 1 absorbs the photon and makes a transition to its final state. All three intermediate states contain a virtual photon. The description of the states mentioned above is summarized in Table I.

The wave functions of the system, consisting of electron 1 and 2 plus nucleus, satisfy the Schrödinger equation (units with $\hbar = m = c = 1$ are used throughout)

$$i \frac{\partial \Phi(\mathbf{R}, t)}{\partial t} = H \Phi(\mathbf{R}, t), \quad (1)$$

where $H = H_0 + H'$ is the Hamiltonian of whole system, H_0 is the unperturbed Hamiltonian of the system, and H' is the interaction of the charged particles with the electromagnetic field and can be written as

$$H' = \int (\mathbf{j}_e + \mathbf{j}_N) \cdot \mathbf{A} d\mathbf{r} \quad (2)$$

where \mathbf{j}_e and \mathbf{j}_N are the current density vectors for electron and nucleus, respectively, and \mathbf{A} is the vector potential of electromagnetic field in the Coulomb gauge. The wave function $\Phi(\mathbf{R}, t)$ can be expanded by the unperturbed wave functions $\Phi_n(\mathbf{R})$ of the system:

$$\Phi(\mathbf{R}, t) = \sum_n C_n(t) \Phi_n(\mathbf{R}). \quad (3)$$

We notice that $H_0 \Phi_n(\mathbf{R}) = E_n \Phi_n(\mathbf{R})$, and E_n is the eigenenergy of the unperturbed system. Table I lists all of the E_n for the numbered unperturbed states concerned. Substitution of (3) into (1) gives

$$i \frac{\partial C_n(t)}{\partial t} = C_n(t) E_n + \sum_{m \neq n} C_m(t) H_{nm}, \quad (4)$$

where $H_{nm} = \langle \Phi_n | H' | \Phi_m \rangle$. In order to solve (4), we make a Laplace transformation for (4) and get

$$ip C_n(p) - i C_n(0) = C_n(p) E_n + \sum_{m \neq n} C_m(p) H_{nm}, \quad (5)$$

with $C_n(p) = \int_0^\infty C_n(t) e^{-ipt} dt$, and $p = \eta - i\omega$. Assuming that the initial conditions of the whole system are $C_1(0) = 1$, $C_m(0) = 0$ ($m \neq 1$), the coefficient equations of the reaction channels can be written as the matrix equation

$$\begin{pmatrix} -ip + E_1 & \int H_{12} dk & \int H_{13} dk & \int H_{14} dk & 0 & 0 \\ H_{21} & -ip + E_2 & 0 & 0 & \int H_{25} dE & H_{26} \\ H_{31} & 0 & -ip + E_3 & 0 & \int H_{35} dE & 0 \\ H_{41} & 0 & 0 & -ip + E_4 & 0 & H_{46} \\ 0 & \int H_{52} dk & \int H_{53} dk & 0 & -ip + E_5 & 0 \\ 0 & \int H_{62} dk & 0 & \int H_{64} dk & 0 & -ip + E_6 \end{pmatrix} \begin{pmatrix} C_1 \\ C_2 \\ C_3 \\ C_4 \\ C_5 \\ C_6 \end{pmatrix} = \begin{pmatrix} -i \\ 0 \\ 0 \\ 0 \\ 0 \\ 0 \end{pmatrix}, \quad (6)$$

TABLE I. Description of states. ϕ and ψ are, respectively, the electron and nuclear wave functions with subscripts i and f referring to the initial and final states and subscripts 1 and 2 referring to electrons 1 and 2. E denotes the energies of electron and nuclear states with subscripts 1, 2, and N referring to electron 1, electron 2, and nucleus. k is the photon energy.

State	e_1	e_2	Nucleus	Photon	Energy	Prob. amp.
Initial	ϕ_{1i}	ϕ_{2i}	ψ_i	0	$E_1 = E_{1i} + E_{2i}$	C_1
Intermediate	ϕ_{1f}	ϕ_{2i}	ψ_i	1	$E_2 = E_{1f} + E_{2i} + k$	C_2
	ϕ_{1i}	ϕ_{2f}	ψ_i	1	$E_3 = E_{1i} + E_{2f} + k$	C_3
	ϕ_{1i}	ϕ_{2i}	ψ_f	1	$E_4 = E_{1i} + E_{2i} + E_{Nf}$	C_4
Final	ϕ_{1f}	ϕ_{2f}	ψ_i	0	$E_5 = E_{1f} + E_{2f}$	C_5
	ϕ_{1f}	ϕ_{2i}	ψ_f	0	$E_6 = E_{1f} + E_{2i} + E_{Nf}$	C_6

where $\int dk$ designates an integral over all continuum energies of the emitted photon, and $\int dE$ denotes an integral over all continuum energies of the Auger electron.

From the initial conditions, C_1 in the zeroth-order approximation is

$$C_1^{(0)} = \frac{i}{ip - E_1} . \quad (7)$$

Substitution of (7) into (6) gives C_2 , C_3 , and C_4 in the first-order approximation

$$C_2^{(1)} = \frac{H_{21}}{ip - E_2} C_1^{(0)} , \quad (8)$$

$$C_3^{(1)} = \frac{H_{31}}{ip - E_3} C_1^{(0)} , \quad (9)$$

$$C_4^{(1)} = \frac{H_{41}}{ip - E_4} C_1^{(0)} . \quad (10)$$

Substituting Eqs. (8), (9), and (10) into (6) yields C_5 and C_6 in the second-order approximation:

$$C_5^{(2)} = \frac{U_A}{ip - E_5} C_1^{(1)} , \quad (11)$$

$$C_6^{(2)} = \frac{U_B}{ip - E_6} C_1^{(1)} , \quad (12)$$

where

$$U_A = \int \frac{H_{52}H_{21}}{ip - E_2} dk + \int \frac{H_{53}H_{31}}{ip - E_3} dk , \quad (13)$$

$$U_B = \int \frac{H_{62}H_{21}}{ip - E_2} dk + \int \frac{H_{64}H_{41}}{ip - E_4} dk . \quad (14)$$

Substitution of (8), (9), and (10) into (6) gives C_1 in the second-order approximation

$$C_1^{(2)} = \frac{i}{ip - E_1 + i\gamma_1} , \quad (15)$$

where

$$\gamma_1 = - \int \frac{iH_{12}H_{21}}{E_2 - ip} dk - \int \frac{iH_{13}H_{31}}{E_3 - ip} dk + \int \frac{iH_{14}H_{41}}{E_4 - ip} dk \quad (16)$$

is the contribution from x-ray emission to the level width of the initial hole state. Substitution of (15), (11), and (12) into (6) gives C_2 , C_3 , and C_4 in the third-order approximation:

$$C_2^{(3)} = \frac{1}{ip - E_2} \left[H_{21} + i\pi U_A H_{25} + \frac{U_B H_{26}}{ip - E_6} \right] C_1^{(2)} , \quad (17)$$

$$C_3^{(3)} = \frac{1}{ip - E_3} (H_{31} + i\pi U_A H_{35}) C_1^{(2)} , \quad (18)$$

$$C_4^{(3)} = \frac{1}{ip - E_4} \left[H_{41} + \frac{U_B H_{46}}{ip - E_6} \right] C_1^{(2)} . \quad (19)$$

Substitution of (17), (18), and (19) into (6) gives C_1 in the fourth-order approximation

$$C_1^{(4)} = \frac{1}{p + iE_1 + \gamma_1 + \gamma_2 + \gamma_3} , \quad (20)$$

where

$$\gamma_2 = \int \frac{\pi H_{12}H_{25}U_A}{E_2 - ip} dk + \int \frac{\pi H_{13}H_{35}U_A}{E_3 - ip} dk \quad (21)$$

is the contribution from the Auger electron emission to the level width of the initial hole state, and

$$\gamma_3 = \int \frac{H_{12}H_{26}U_B}{(E_2 - ip)(p + iE_6)} dk + \int \frac{H_{14}H_{46}U_B}{(E_4 - ip)(p + iE_6)} dk \quad (22)$$

is the contribution from the NEET process to the level width of the initial hole state. Finally, substitution of (20) into (17), (11), and (12) gives

$$C_2^{(5)} = \frac{1}{ip - E_2} \left[H_{21} + i\pi U_A H_{25} + \frac{U_B H_{26}}{ip - E_6} \right] \times \frac{1}{p + iE_1 + \gamma_1 + \gamma_2 + \gamma_3} , \quad (23)$$

$$C_5^{(5)} = \frac{U_A}{ip - E_5} \frac{1}{p + iE_1 + \gamma_1 + \gamma_2 + \gamma_3} , \quad (24)$$

$$C_6^{(5)} = \frac{U_B}{ip - E_6} \frac{1}{p + iE_1 + \gamma_1 + \gamma_2 + \gamma_3} . \quad (25)$$

We now make the Laplace inverse transforms for (20), (23), (24), and (25), and get

$$C_1(t) = e^{-iE_1 t} e^{-(\gamma_1 + \gamma_2 + \gamma_3)t} , \quad (26)$$

$$\begin{aligned} C_2(t) &= \frac{H_{21}}{(E_2 - E_1) + i(\gamma_1 + \gamma_2 + \gamma_3)} [e^{-iE_2 t} - C_1(t)] + \frac{i\pi U_A H_{25}}{(E_2 - E_1) + i(\gamma_1 + \gamma_2 + \gamma_3)} [e^{-iE_2 t} - C_1(t)] \\ &\quad + \frac{U_B H_{26}}{(E_6 - E_2)[(E_6 - E_1) + i(\gamma_1 + \gamma_2 + \gamma_3)][(E_2 - E_1) + i(\gamma_1 + \gamma_2 + \gamma_3)]} \\ &\quad \times \{ [(E_6 - E_1) + i(\gamma_1 + \gamma_2 + \gamma_3)] e^{-iE_2 t} + [(E_2 - E_1) + i(\gamma_1 + \gamma_2 + \gamma_3)] e^{-iE_6 t} + (E_6 - E_2) C_1(t) \} \\ &= C_2^{(1)}(t) + C_2^{(2)}(t) + C_3^{(3)}(t) , \end{aligned} \quad (27)$$

$$C_5(t) = \frac{U_A}{(E_5 - E_1) + i(\gamma_1 + \gamma_2 + \gamma_3)} [e^{-iE_5 t} - C_1(t)], \quad (28)$$

$$C_6(t) = \frac{U_B}{(E_6 - E_1) + i(\gamma_1 + \gamma_2 + \gamma_3)} [e^{-iE_6 t} - C_1(t)], \quad (29)$$

where $C_2^{(1)}(t)$, $C_2^{(2)}(t)$, and $C_2^{(3)}(t)$ in (27) denote the three terms between the two equal signs in (27), respectively. Because γ_1 , γ_2 , and γ_3 are real and positive, we have

$$|C_1(t)|^2 = e^{-2(\gamma_1 + \gamma_2 + \gamma_3)t} \xrightarrow{t \rightarrow \infty} 0. \quad (30)$$

The probabilities of the three decay channels can be written

$$P_{\text{xray}} = \int_0^\infty |C_2(\infty)|^2 dk = \int_0^\infty |C_2^{(1)}(\infty) + C_2^{(2)}(\infty) + C_2^{(3)}(\infty)|^2 dk, \quad (31)$$

$$P_{\text{Auger}} = \int_0^\infty |C_5(\infty)|^2 dk = \frac{\pi}{\gamma_1 + \gamma_2 + \gamma_3} |U_A|^2, \quad (32)$$

$$P_{\text{NEET}} = |C_6(\infty)|^2 = \frac{1}{(E_6 - E_1)^2 + (\gamma_1 + \gamma_2 + \gamma_3)^2} |U_B|^2. \quad (33)$$

To explore the physical significance of (31), let us consider the first term in (31) [11].

$$\begin{aligned} \int_0^\infty |C_2^{(1)}(\infty)|^2 dk &= \lim_{t \rightarrow \infty} \int_0^\infty \left| \frac{H_{21}}{(E_2 - E_1) + i(\gamma_1 + \gamma_2 + \gamma_3)} [e^{-iE_2 t} - C_1(t)] \right|^2 dk \\ &= \frac{\pi}{\gamma_1 + \gamma_2 + \gamma_3} |H_{21}|^2 = \frac{\gamma_1}{\gamma_1 + \gamma_2 + \gamma_3}. \end{aligned} \quad (34)$$

Obviously, this term corresponds to the conventional probability of x-ray emission. The second term in (31) contains the matrix element H_{25} , which represents the transition from the Auger electron state to the final state of x-ray emission. The third term in (31) contains the matrix element H_{26} , which represents the nuclear transition from the nuclear excited state to the ground state with an emission of x-ray. Therefore, the second and third terms in (31) represent the interference effects due to the presence of the Auger electron and nuclear excitation, respectively, upon the x-ray emission channel.

III. NUMERICAL CALCULATIONS

To make numerical calculations, we first simplify the expressions (31), (32), and (33). Because the NEET probability is extremely small as compared with the probabilities of x-ray and Auger electron emissions, it is appropriate to neglect the contribution from the NEET process to the level width of the initial hole state. Furthermore, because the Auger electron emission and NEET process correspond to the second-order perturbation processes, while the x-ray emission is the only one of the first-order perturbed processes, we neglect the interference effects from the former two processes to the x-ray emission in the numerical evaluations. Then, (31), (32), and (33) can be simplified as follows:

$$P_{\text{xray}} = \frac{\gamma_1}{\gamma_1 + \gamma_2}, \quad (35)$$

$$P_{\text{Auger}} = \frac{\gamma_2}{\gamma_1 + \gamma_2}, \quad (36)$$

$$P_{\text{NEET}} = \frac{|U_B|^2}{(E_6 - E_1)^2 + (\gamma_1 + \gamma_2)^2}. \quad (37)$$

We now turn to the treatments of the interaction matrix elements. We adopt the standard technique in the electromagnetic transition theory for the calculations of these matrix elements and restrict ourself to study transitions from a k -shell hole state to adjacent main shells. The matrix elements of x-ray processes for an electric dipole transition are given by

$$\begin{aligned} \gamma_1 &= \frac{2}{3} \frac{(2j_{1f} + 1)}{(2j_{1i} + 1)} \Delta E (C_{j_{1f} 1/2 L 0}^{j_{1i} 1/2})^2 \\ &\times \left| \int_0^\infty R_{1i}(r) R_{1f}(r) j_1(kr) r^2 dr \right|^2, \end{aligned} \quad (38)$$

where $j_{1i(f)}$ denotes the total angular momentums of the electron states, $R_{1i(f)}$ designates the electron radial wave functions, $k = \Delta E = E_{1f} - E_{1i}$, $C_{j_{1f} 1/2 L 0}^{j_{1i} 1/2}$ is the Clebsch-Gordan coefficient, and $j_1(kr)$ is the spherical Bessel function of first order. As for the Auger emission, we use antisymmetric wave functions for the two indistinguishable electrons. Also, we consider only the electric dipole transition and Auger emission of type (KLL). Then we have

$$\begin{aligned}
U_A = & \frac{4\pi}{3} \sqrt{(2j_{1f}+1)(2j_{2f}+1)} \left[(-1)^{J_f+j_{2f}+j_{1i}} \begin{Bmatrix} j_{1f} & j_{2f} & J_f \\ j_{2i} & j_{1i} & 1 \end{Bmatrix} \delta_{J_i J_f} \delta_{M_i M_f} \langle J_{1f} \| Y_1 \| j_{1i} \rangle \langle j_{2f} \| Y_1 \| j_{2i} \rangle \right. \\
& \left. - (-1)^{J_f+j_{2f}+j_{2i}} \begin{Bmatrix} J_{1f} & J_{2f} & J_f \\ j_{1i} & j_{2i} & 1 \end{Bmatrix} \delta_{J_i J_f} \delta_{M_i M_f} \langle j_{1f} \| Y_1 \| j_{2i} \rangle \langle j_{2f} \| Y_1 \| j_{1i} \rangle \right] \\
& \times \left[\int_0^\infty R_{2i}(r_2) R_{2f}(r_2) dr_2 \int_0^{r_2} R_{1i}(r_1) R_{1f}(r_1) r_1^3 dr_1 + \int_0^\infty R_{2i}(r_2) R_{2f}(r_2) r_2^3 dr_2 \int_{r_2}^\infty R_{1i}(r_1) R_{1f}(r_1) dr_1 \right], \quad (39)
\end{aligned}$$

where $j_{1i(f)}$ and $j_{2i(f)}$ denote the total spins of the concerned electron states, $J_{i(f)}$ and $M_{i(f)}$ are, respectively, the quantum numbers of the total angular momentum and projections of the two-electron system, and

$$\begin{Bmatrix} j_{1f} & j_{2f} & J_f \\ j_{2i} & j_{1i} & 1 \end{Bmatrix}$$

is Wigner 6j symbol. It is readily verified that [11]

$$\gamma_2 = \pi |U_A|^2. \quad (40)$$

Now we turn to calculate the NEET matrix element

$$U_B = (-1)^{J_f+j_{1f}+I_i} \begin{Bmatrix} I_i & j_{1i} & J_f \\ j_{1f} & I_f & L \end{Bmatrix} \delta_{J_i J_f} \delta_{M_i M_f} \sqrt{(2j_{1f}+1)(2I_f+1)} \times \langle I_f \| M_L^q(r_N) \| I_i \rangle \langle j_{1f} \| N_L^q(r_e) \| j_{1i} \rangle, \quad (41)$$

where $j_{1i(f)}$ and $I_{i(f)}$ are, respectively, the total angular momenta of the electron and nucleus, $J_{i(f)}$ and $M_{i(f)}$ designate the total angular momenta and their projections of the electron-nucleus system, while $\langle I_f \| M_L^q(r_N) \| I_i \rangle$ and $\langle j_{1f} \| N_L^q(r_e) \| j_{1i} \rangle$ are, respectively, the nuclear and electron reduced transition matrix elements [$q=E(M)$ denotes the electric (magnetic) transition]. The reduced nuclear matrix element is defined [12] by

$$\langle I_f \mu_f \| M_{L\mu}^q(r_N) \| I_i \mu_i \rangle = C_{I_i \mu_i L \mu}^{I_f \mu_f} \langle I_f \| M_L^q(r_N) \| I_i \rangle. \quad (42)$$

The reduced matrix element may be related to the measured lifetime of the excited nuclear level by

$$|\langle I_f \| M_L^q(r_N) \| I_i \rangle|^2 = \frac{L[(2L+1)!!]^2}{8\pi(L+1)\Delta E^{2L+1}} \frac{1}{\tau} \quad (43)$$

where $\Delta E = E_{Nf} - E_{Ni}$ is the energy difference between nuclear levels. It should be noted that in Eq. (43) the quantity τ corresponds to a decay process ($f \rightarrow i$), whereas the reduced matrix element refers to an excitation process ($i \rightarrow f$). Recalling Eq. (42), one has

$$|\langle I_f \| M_L^q(r_N) \| I_i \rangle|^2 = \frac{2I_i+1}{2I_f+1} |\langle I_i \| M_L^q(r_N) \| I_f \rangle|^2. \quad (44)$$

With regard to the electron reduced matrix element for an electric 2^L -pole transition, we have

$$|\langle j_{1f} \| N_L^E(r_e) \| j_{1i} \rangle|^2 = \frac{4\pi e^2 (2j_{1i}+1)(2l_{1i}+1)}{2L+1} \left[\begin{Bmatrix} l_{1i} & j_{1i} & 1/2 \\ j_{1f} & l_{1f} & L \end{Bmatrix} \right]^2 (C_{l_{1i} 0 L 0}^{l_{1f} 0})^2 \left[\int \mathcal{R}_{1f}(r) r^{-(L-1)} \mathcal{R}_{1i}(r) dr \right]^2, \quad (45)$$

where, \mathcal{R} 's are the radial wave functions of the bound electrons. For a magnetic dipole transition the electron reduced matrix element is

$$\begin{aligned}
|\langle j_{1f} \| N_L^{M^1}(r_e) \| j_{1i} \rangle|^2 = & (2\mu_B)^2 \left[\frac{2}{\sqrt{3}} \delta_{l_{1i} 0} \delta_{l_{1f} 0} \mathcal{R}_{1i}(0) \mathcal{R}_{1f}(0) \right. \\
& \left. + \int \mathcal{R}_{1f}(r) \frac{1}{r} \mathcal{R}_{1i}(r) dr \left[\delta_{l_{1i} l_{1f}} (-1)^{1/2-l_{1f}-j_{1f}} \right. \right. \\
& \left. \left. \times \sqrt{l_{1i}(l_{1i}+1)(2l_{1i}+1)(2j_{1i}+1)} \begin{Bmatrix} l_{1i} & j_{1i} & 1/2 \\ j_{1f} & l_{1f} & 1 \end{Bmatrix} \right. \right. \\
& \left. \left. + 3\sqrt{5} \sqrt{(2l_{1i}+1)(2j_{1i}+1)} C_{l_{1i} 0 2 0}^{l_{1f} 0} \begin{Bmatrix} l_{1f} & 1/2 & j_{1f} \\ l_{1i} & 1/2 & j_{1i} \\ 2 & 1 & 1 \end{Bmatrix} \right] \right]^2, \quad (46)
\end{aligned}$$

where μ_B is the Bohr magneton, $\mathcal{R}(0)$ is the value of electron radial wave function at the origin, and

$$\begin{pmatrix} a & b & c \\ d & e & f \\ g & h & i \end{pmatrix}$$

is the Wigner $9j$ symbol. The readers are referred to Ref. [7] for detailed treatments of the interaction matrix elements [13].

We also calculate the upper limits of the NEET process. Assuming the energy difference of electron levels matches perfectly with that of the nuclear levels, the upper limit can be determined by

$$P_{\max} = \frac{|U'_B|^2}{(\gamma_1 + \gamma_2)^2}, \quad (47)$$

where the nuclear reduced transition matrix elements are estimated with the Weisskopf unit.

Using (35)–(47), we calculate the decay probabilities of various channels for the nuclei $^{189}_{76}\text{Os}$, $^{197}_{79}\text{Au}$, and $^{237}_{93}\text{Np}$. The atomic and nuclear level diagrams studied and the transition multipolarities for the NEET process are shown in Fig. 2. In the calculations, the nuclear reduced matrix elements are evaluated by Eq. (43) with the experimentally measured lifetime of the excited states. This procedure could benefit us by relying on any approximate nuclear model. The relevant lifetime data are listed in Table II. In calculating the reduced electron transition matrix elements from (45) and (46), the hydrogenlike electron wave function has been adopted with an effective nuclear charge Z' to account for the shielding effect of inner-shell electrons. For example, in the event of

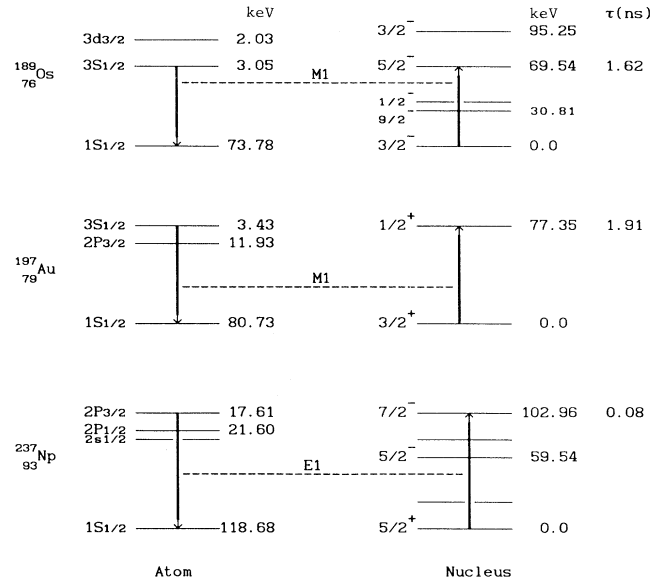


FIG. 2. NEET diagrams. The atomic levels are taken from Ref. [14]. The nuclear levels are taken from Refs. [15] (^{189}Os), [16] (^{197}Au), and [17] (^{237}Np), respectively, τ is the level lifetime.

$3S_{1/2} \rightarrow 1S_{1/2}$ transition in $^{189}_{76}\text{Os}$, the initial electron wave function is $\mathcal{R}_{1i}(r) = \mathcal{R}_{30}^H(z', r)$ with $z' = 76 - 10 = 66$ and $\mathcal{R}_{1f}(r) = \mathcal{R}_{10}^H(z', r)$ with $z' = 76$, where $\mathcal{R}_{nl}^H(z', r)$ is the hydrogenlike wave function with quantum numbers (n, l) and effective charge Z' . This occurs because the total number of the electrons in the inner-shell $n = 1$ and $n = 2$ is ten. The calculated results are listed in Table II, where

TABLE II. Calculated values for x-ray, Auger electron, and NEET processes and measured data. $\Delta E = (E_{1f} - E_{1i}) - (E_{nf} - E_{ni})$ is the energy difference between atomic and nuclear levels [14–17]. τ is the lifetime of the nuclear level [15–17]. γ_1 and γ_2 are, respectively, the partial transition widths of x-ray and Auger electron emissions (the corresponding experimental data are taken from Ref. [18]). P 's are probabilities for various decay channels. Th refers to theoretical, and Ex to experimental. An asterisk denotes the present work, and a dagger is the calculated upper limit of NEET probability P_{\max} .

	ΔE (eV)	NEET multip.	τ (s)	γ_1 (eV)		γ_2 (eV)		P_{xray}	P_{Auger}	P_{NEET}		
				Th	Ex	Th	Ex			Th	Ex	
$^{189}_{76}\text{Os}$	1261.5	M1	1.64	20.77	20.0	0.55	0.75	0.97	0.03	1.5×10^{-7} [2]	$(1.7 \pm 0.2) \times 10^{-7}$ [19]	
										2.5×10^{-7} [3]		
										1.1×10^{-7} [4]		$(4.3 \pm 0.2) \times 10^{-8}$ [20]
										2.31×10^{-7} [5]		$(5.7 \pm 1.7) \times 10^{-9}$ [21]
										3.4×10^{-10} [6]		$\cong 10^{-6}$ [22]
										$2.1 \times 10^{-9*}$		
$^{197}_{79}\text{Au}$	74.18	M1	1.91	24.15	27.5	0.57	0.9	0.98	0.02	$1.5 \times 10^{-3\dagger}$	$(2.2 \pm 1.8) \times 10^{24}$ [23]	
										3.5×10^{-5} [3]		
										2.2×10^{-5} [5]		
										1.3×10^{-7} [6]		
										$2.4 \times 10^{-7*}$		
$^{237}_{93}\text{Np}$	1902	E1	0.08	47.5	50.0	0.62	1.1	0.99	0.01	$2.4 \times 10^{-3\dagger}$	$(2.1 \pm 0.6) \times 10^{-4}$ [24]	
										1.5×10^{-7} [3]		
										2.6×10^{-4} [5]		
										3.1×10^{-12} [6]		
										$1.9 \times 10^{-9*}$		
										$4.1 \times 10^{-3\dagger}$		

the available experimental data and other theoretical results are also presented for a comparison. From Table II, one may find that there exist great discrepancies among the experimental and theoretical NEET results.

IV. SUMMARY AND DISCUSSION

Collecting our main results, we have the following.

(1) Based upon a unified framework of nonrelativistic quantum mechanics theory, the self-consistent descriptions of the transition probabilities for x-ray emission, Auger electron emission, and the NEET process are presented in (31), (32), and (33). It appears that the interference effects between NEET and the other two processes are negligible because of the great difference in magnitude between the NEET matrix element and the other processes.

(2) Since the main goal of this work is to study the NEET process, including its relationship with x-ray and Auger electron emissions and evaluation of the magnitude of order of the transition probability, it is reasonable to make use of some approximations in the present calculations, such as the nonrelativistic, point nuclear model and hydrogenlike wave functions, etc. These approximations are certainly insufficient for accurate calculations of Auger electron and x-ray emissions.

(3) Using the simplified formulas (35), (36), and (37), the transition probabilities of the three processes for the nuclei ^{189}Os , ^{197}Au , and ^{237}Np are calculated and compared with the available experimental and other theoretical results. Compared to the previous calculations [7] on NEET probabilities, we have made some improvement in the present work. The evaluation of the reduced nuclear transition matrix element has been corrected [13]. We introduce the effective charge in the hydrogenlike wave functions to account for the multielectron effect. In addition, we have tested the impact on calculated NEET probability by taking into account some other effects. One of these is the use of the retarded interaction between two point charges

$$\frac{e^{ik|\mathbf{r}_e - \mathbf{r}_N|}}{|\mathbf{r}_e - \mathbf{r}_N|}$$

instead of the static interaction

$$\frac{1}{|\mathbf{r}_e - \mathbf{r}_N|}.$$

By using the equality [25]

$$\frac{e^{ik|\mathbf{r}_e - \mathbf{r}_N|}}{|\mathbf{r}_e - \mathbf{r}_N|} = 4\pi ik \sum_{L=0}^{\infty} j_L(kr_N) h_L^{(1)}(kr_e) \times \sum_{m=-L}^L Y_{Lm}^*(\hat{\mathbf{r}}_N) Y_{Lm}(\hat{\mathbf{r}}_e), \quad (48)$$

where $h_L^{(1)}(kr_e)$ is the spherical Hankel function of the first kind, the radial integral in Eq. (45) has now become

$$\int \mathcal{R}_{1f}(r) h_L^{(1)}(kr) \mathcal{R}_{1i}(r) r^2 dr,$$

rather than

$$\int \mathcal{R}_{1f}(r) r^{-(L-1)} \mathcal{R}_{1i}(r) dr.$$

The numerical results calculated from these two radial integrals show a 10% difference. Also, we have examined the interference effect from nearby nuclear and atomic levels. For instance, in the case of ^{189}Os , in addition to the marked electron transition $3S_{1/2}(3.073 \text{ keV}) \rightarrow 1S_{1/2}(73.875 \text{ keV})$ (see Fig. 2), the transition from the nearby level $3d_{3/2}(2.043 \text{ keV})$ to $1S_{1/2}(73.875 \text{ keV})$ is also a $M1$ transition in nature, thus it could interfere with the former. We have found that by taking account of all these effects, the calculated NEET probabilities are still far from the measured data, especially for the nuclei ^{197}Au and ^{237}Np . We also notice the large differences among the measured NEET data in ^{189}Os from different laboratories [19-22]. More accurate measurements are desirable to identify the origins of these discrepancies.

-
- [1] M. Morita, *Progr. Theor. Phys.* **49**, 1547 (1973).
 [2] K. Okamoto, *Laser Interactions and Related Plasma Phenomena* (Plenum, New York, 1977), Vol. 4A, p. 283.
 [3] K. Pisk, Z. Kaliman, and B. A. Logan, *Nucl. Phys.* **A504**, 103 (1989).
 [4] M. D. Bondar'kov and V. M. Kolomiets, *Izv. Akad. Nauk SSSR, Ser. Fiz.* **55**, 983 (1991).
 [5] A. Ljubicic, K. Kekez, and B. A. Logan, *Phys. Lett. B* **272**, 1 (1991).
 [6] E. V. Tkalya, *Zh. Eksp. Teor. Fiz.* **102**, 379 (1992) [*Sov. Phys. JETP* **75**, 200 (1992)].
 [7] Yu-kun Ho, Bao-hui Zhang, and Zhu-sou Yuan, *Phys. Rev. C* **44**, 1910 (1991).
 [8] E. V. Tkalya, *Nucl. Phys.* **A539**, 209 (1992).
 [9] W. Bambynek *et al.*, *Rev. Mod. Phys.* **44**, 716 (1972).
 [10] M. H. Chen, "Relativistic Calculation of Atomic Transition Probabilities," in *Atomic Inner-shell Physics*, edited by B. Crasemann (Plenum, New York, 1985), p. 31.
 [11] N. Tralli and G. Goertzel, *Phys. Rev.* **83**, 399 (1951).
 [12] M. E. Rose, *Elementary Theory of Angular Momentum* (Wiley, New York, 1957).
 [13] In Eq. (10) of Ref. [7], the factor $C_{i_{0L}^0}^{j_{f_{0L}^0}}$ was missing. Also, the difference between the two kinds of reduced matrix elements shown in Eq. (44) of this paper was overlooked in Ref. [7]. We have corrected these two points in this article.
 [14] K. N. Huang, *At. Data Nucl. Data Tables* **18**, 243 (1976).

- [15] R. B. Firestone, Nucl. Data Sheets **59**, 869 (1990).
- [16] B. Harmatz, Nucl. Data Sheets **34**, 101 (1981).
- [17] Y. A. Ellis-Akovi, Nucl. Data Sheets **49**, 181 (1986).
- [18] O. K. Rahkonen and M. O. Krause, At. Data Nucl. Data Tables **14**, 139 (1974).
- [19] K. Otozai, R. Arakawa, and T. Saito, Nucl. Phys. **A297**, 97 (1978).
- [20] T. Saito, A. Shinohara, T. Miura, and K. Otozai, J. Inorg. Nucl. Chem. **43**, 1963 (1981).
- [21] A. Shinohara *et al.*, Nucl. Phys. **A472**, 151 (1987).
- [22] K. Otozai, R. Arakawa, and M. Morita, Prog. Theor. Phys. **50**, 1771 (1973).
- [23] H. Fujioka *et al.*, Z. Phys. A **315**, 121 (1984).
- [24] T. Saito, A. Shinohara, and K. Otozai, Phys. Lett. **92B**, 293 (1980).
- [25] J. D. Jackson, *Classical Electrodynamics* (Wiley, New York, 1976).